Available online at www.sciencedirect.com
ScienceDirect
Journal of Nuclear Materials 367–370 (2007) 377–381
journal of nuclear materials
www.elsevier.com/locate/jnucmat

Microstructural investigation, using small-angle neutron scattering (SANS), of Optifer steel after low dose neutron irradiation and subsequent high temperature tempering

R. Coppola [a,*], R. Lindau [b], M. Magnani [c,1], R.P. May [d], A. Möslang [b], M. Valli [c]

[a] *ENEA-Casaccia, FPN, CP 2400, 00100 Roma, Italy*
[b] *Forschungszentrum Karlsruhe, IMF-I, P.O. Box 3640, D-76021 Karlsruhe, Germany*
[c] *ENEA-'Clementel', FIM, V. Don Fiammelli 2, 40129 Bologna, Italy*
[d] *Institut Max von Laue – Paul Langevin, 6, rue Jules Horowitz, 38042 Grenoble, France*

Abstract

The microstructural effect of low dose neutron irradiation and subsequent high temperature tempering in the reduced activation ferritic/martensitic steel Optifer (9.3 Cr, 0.1 C, 0.50 Mn, 0.26 V, 0.96 W, 0.66 Ta, Fe bal wt%) has been studied using small-angle neutron scattering (SANS). The investigated Optifer samples had been neutron irradiated, at 250 °C, to dose levels of 0.8 dpa and 2.4 dpa. Some of them underwent 2 h tempering at 770 °C after the irradiation. The SANS measurements were carried out at the D22 instrument of the High Flux Reactor at the Institut Max von Laue – Paul Langevin, Grenoble, France. The differences observed in nuclear and magnetic SANS cross-sections after subtraction of the reference sample from the irradiated one suggest that the irradiation and the subsequent post-irradiation tempering produce the growth of non-magnetic defects, tentatively identified as microvoids.

1. Introduction

Under neutron irradiation complex microstructural phenomena occur in ferritic/martensitic steels for future fusion reactors and for accelerator driven systems (ADS), implying changes in precipitate composition and the growth of helium bubbles and microvoids, with consequent changes in the thermo-mechanical properties [1–3]. Such steels must therefore be optimised to improve the resistance to swelling and helium effects and their microstructural stability under high temperature irradiation. The microstructural phenomena underlying the changes under irradiation in the ductile-to-brittle transition temperature (DBTT) [4,5] require a careful investigation: techniques such as transmission electron microscopy (TEM) and small-angle neutron scattering (SANS) are quite useful in this regard. SANS allows to distinguish non-magnetic defects, such as microvoids or helium bubbles, and magnetic ones, such as certain kinds of precipitates;

* Corresponding author. Tel.: +39 0 630484724; fax: +39 0 630484747.
E-mail address: coppolar@casaccia.enea.it (R. Coppola).
[1] Now on retirement.

0022-3115/$ - see front matter © 2007 Elsevier B.V. All rights reserved.
doi:10.1016/j.jnucmat.2007.03.125

additional and unique information on defect composition can be obtained using polarised SANS [6–9]. This contribution presents new results of a SANS study carried out to investigate the microstructural effect of neutron irradiation and subsequent tempering in a reduced activation ferritic/martensitic steel of interest for fusion technology.

2. Material characterization

The Optifer steel was investigated, having the following chemical composition: 9.3 Cr, 0.1 C, 0.50 Mn, 0.26 V, 0.96 W, 0.066 Ta Fe bal (wt%) [10–12]. Both the irradiated and the reference samples had been submitted to the standard metallurgical treatment (950 °C for 30 min then 750 °C for 2 h).

The samples were irradiated by exposure to thermal neutrons at the High Flux Reactor – Petten up to dose levels of 0.8 and 2.4 dpa (displacement per atom) at 250 °C. Some of these samples were tempered 2 h at 770 °C after the irradiation. Unirradiated reference samples, submitted to the same thermal treatments as the irradiated ones, were also prepared. The size of both the irradiated and unirradiated specimens utilized for the SANS experiments was $4 \times 10\ \text{mm}^2$ in surface and 1 mm in thickness. The results of TEM observations of these Optifer samples [11] show that after irradiation α'-precipitates (Cr-rich phase), dislocation loops, microvoids and helium bubbles are locally present between the lath boundaries, which appear decorated with carbides such as $(\text{Fe, Cr, V, W})_{23}\text{C}_6$ or TaC, in different contents depending on the irradiation conditions and on the composition of the material. However it is difficult to obtain quantitative information from such local observations, limited both in statistics and because of the TEM resolution in such magnetic materials.

3. Experimental technique

Reference is made to [13,14] and to previous works [6–9] for a general presentation of SANS and of its application to the study of martensitic steels. SANS measurements were carried out using the D22 diffractometer at the Institut Max von Laue – Paul Langevin (ILL), in Grenoble. In a first series of SANS measurements, using a polarised neutron beam, the 0.8 dpa irradiated Optifer samples were investigated, obtaining the results reported in [6,8]. The experimental conditions defined for investigating the 2.4 dpa irradiated Optifer samples, with unpolarised neutron beam, were a neutron wavelength λ of 6 Å and a sample-to-detector distance of 2 m. Defining the scattering vector $Q = 4\pi \sin\theta/\lambda$, where 2θ is the scattering angle and λ the neutron wavelength, Q values ranging between 0.03 Å^{-1} and 0.2 Å^{-1} were obtained, corresponding in the real space to particle sizes between approximately 10 and 100 Å. After correction for background noise, detector efficiency, and attenuation factor the SANS cross-section in physical units (cm^{-2} sterad^{-1}) was obtained by a calibration of the neutron flux, measuring water in a quartz cell, and by means of the ILL standard programs [15]. The SANS cross-section of each reference samples was subtracted from the SANS cross-section of the corresponding irradiated sample, in order to distinguish as accurately as possible the effect of the irradiation itself from all the other microstructural effects arising during the heating at 250 °C for a duration corresponding to the irradiation time.

In the case of magnetic samples, the total SANS cross-section $\mathrm{d}\Sigma(Q)/\mathrm{d}\Omega$ (where Ω stands for the solid angle) can be written as

$$\mathrm{d}\Sigma(Q)/\mathrm{d}\Omega = \mathrm{d}\Sigma(Q)/\mathrm{d}\Omega_{\text{nucl}} + \mathrm{d}\Sigma(Q)/\mathrm{d}\Omega_{\text{mag}} \sin^2\alpha, \tag{1}$$

where $\mathrm{d}\Sigma(Q)/\mathrm{d}\Omega_{\text{nucl}}$ and $\mathrm{d}\Sigma(Q)/\mathrm{d}\Omega_{\text{mag}}$ are the nuclear and magnetic SANS cross-sections respectively and α is the azimuthal angle on the detector plane. A saturating horizontal magnetic field of 1 T was applied perpendicular to the incoming neutron beam in order to distinguish $\mathrm{d}\Sigma(Q)/\mathrm{d}\Omega_{\text{nucl}}$ and $\mathrm{d}\Sigma(Q)/\mathrm{d}\Omega_{\text{mag}}$, so that only nuclear scattering occurs in the horizontal plane, while nuclear and magnetic scattering occur in the vertical one (the purely magnetic scattering is obtained as the difference between the vertical and horizontal SANS cross-sections).

The nuclear plus magnetic to nuclear cross-sections ratio $R(Q)$ (also defined as 'A' in the literature) can be written as

$$\begin{aligned} R(Q) &= (\mathrm{d}\Sigma(Q)/\mathrm{d}\Omega_{\text{nucl}} + \mathrm{d}\Sigma(Q)/\mathrm{d}\Omega_{\text{mag}})/\mathrm{d}\Sigma(Q)/\mathrm{d}\Omega_{\text{nucl}} \\ &= 1 + (\Delta\rho)^2_{\text{m}}(\Delta\rho)^2_{\text{n}}, \end{aligned} \tag{2}$$

where $(\Delta\rho)^2_{\text{m}}$ and $(\Delta\rho)^2_{\text{n}}$ are respectively the neutron magnetic and nuclear scattering length density square differences between matrix and the microstructural inhomogeneities giving rise to the observed SANS effect to [13,14]. In complex steels, such as Optifer, inhomogeneities with different

chemical composition and size are generally present after irradiation, reflecting a more or less marked dependence on Q of the $R(Q)$ ratio; if $R(Q)$ is constant in Q a homogeneous defect composition can be assumed.

The size distributions were determined by indirect transformation of the SANS cross-section

$$d\Sigma(Q)/d\Omega = (\Delta\rho)^2 \int_0^\infty dR N(R) V^2(R) |F(Q,R)|^2, \quad (3)$$

where $N(R)$ is the number per unit volume of centers with a typical size between R and $R + dR$ (the volume distribution function is $D(R) = N(R)R^3$, V their volume and $|F(Q,R)|^2$ their form factor (assumed spherical in this case) and $(\Delta\rho)^2$ is the 'contrast' or square difference in neutron scattering length density between the inhomogeneities and the metallic matrix [6,8]. Eq. (3) was solved using the method reported in ref. [16] and more recently discussed in Ref. [17].

4. Results and discussion

As shown in Refs. [6,8] after irradiation at 0.8 dpa no difference is detectable within the experimental uncertainties between the irradiated and the reference Optifer sample. After subsequent tempering at 770 °C a slight increase in the nuclear and nuclear plus magnetic SANS cross-section of the irradiated sample with respect to the reference one is observed, but no change can be detected either in the respective $R(Q)$ ratios or in the interference terms. This is consistent with the fact that the volume fraction of the defects produced for such a low irradiation dose in this steel [11] is too low for being observed by SANS. After irradiation to 2.4 dpa a consistent increase in the SANS cross-sections of the irradiated Optifer sample with respect to the reference one is observed, as shown in Fig. 1(a), indicating a high density of irradiation defects in the size range between 10 and 30 Å. Fig. 1(b) shows that for these same two samples the corresponding $R(Q)$ ratio is substantially changed after irradiation. Namely, in the reference sample the $R(Q)$ values indicate the presence of carbide precipitates such as the $(Cr, Fe)_{23}C_6$ [6,17], possibly produced during the initial metallurgical treatment of the as-received material. After irradiation $R(Q)$ is nearly constant, suggesting that the microstructural defects produced under irradiation have a homogeneous chemical composition. Tempering 2 h at 770 °C after the irradiation produces an increase in the SANS cross-sections of the irradiated sample with respect to the reference one (Fig. 2(a)), much smaller than in the case of the as-irradiated sample, but leaves almost unchanged the $R(Q)$ ratio (Fig. 2(b)), very close to the values measured for the unirradiated reference sample (Fig. 1(b)). That suggests that both in the reference and in the irradiated sample the post-irradiation tempering promotes the growth of carbide precipitates in the martensitic matrix. The small difference between the SANS cross-sections of the irradiated and of the reference sample is tentatively attributed to the fact that the small non-magnetic inhomogeneities observed just after irradiation, grow to much larger sizes under the effect of the tempering, giving rise to a SANS effect outside the experimentally available Q window. All these features are more clearly visible in Fig. 3(a) and (b), showing the nuclear SANS cross-section and the $R(Q)$ ratio obtained for the difference between the irradiated and the reference sample, both in

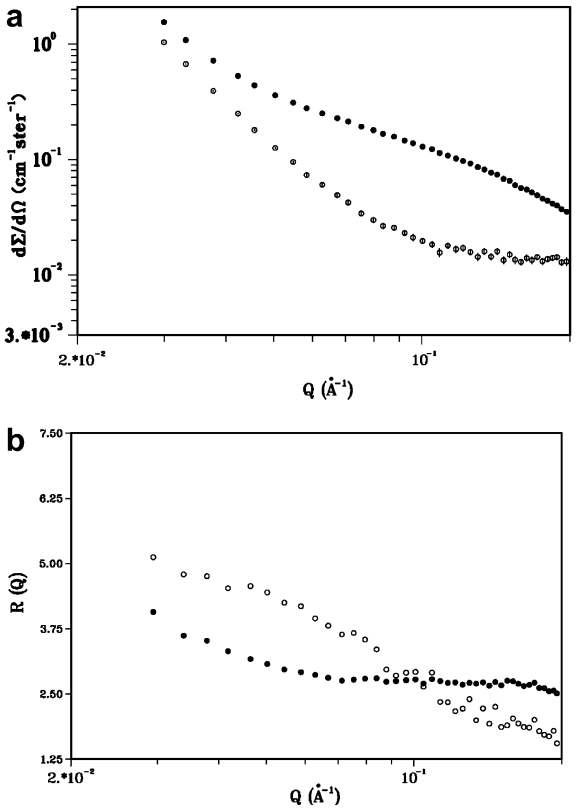

Fig. 1. Optifer samples irradiated with 2.4 dpa at 250 °C (full dots) and reference (empty dots). (a) Nuclear SANS cross-sections and (b) $R(Q)$.

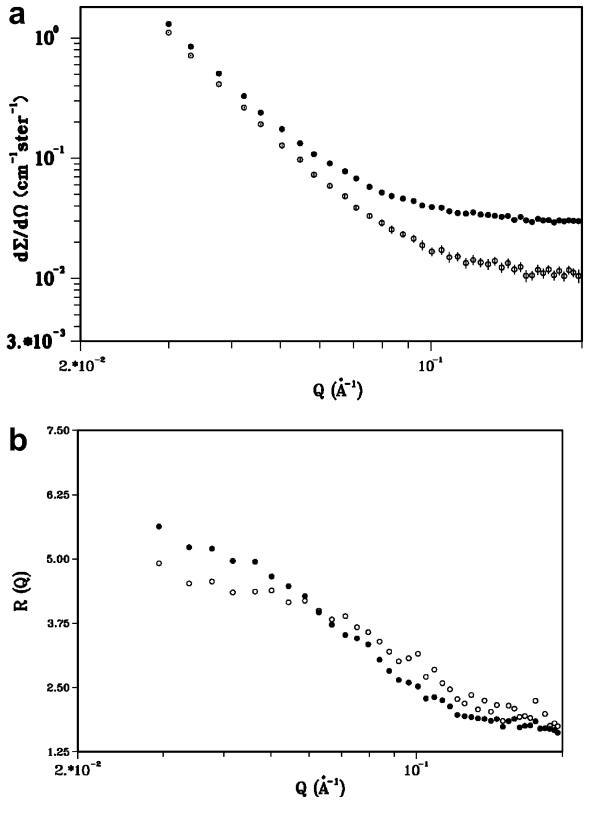

Fig. 2. Optifer samples irradiated with 2.4 dpa at 250 °C then tempered 2 h at 700 °C (full dots) and reference (empty dots). (a) Nuclear SANS cross-sections and (b) $R(Q)$.

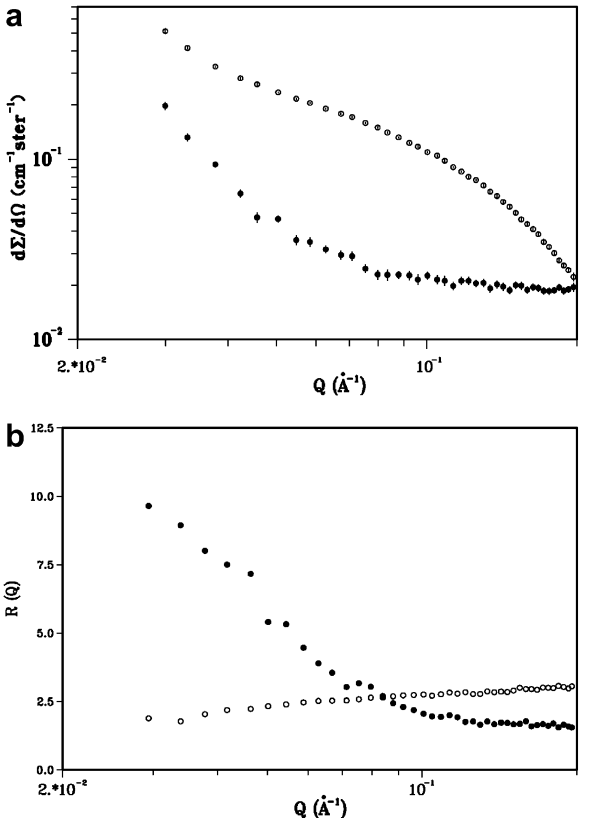

Fig. 3. Difference between irradiated (empty dots irradiated with 2.4 dpa at 250 °C, full dots irradiated with 2.4 dpa at 250 °C then tempered 2 h at 770 °C) and reference Optifer samples. (a) Nuclear SANS cross-sections and (b) $R(Q)$.

the as-irradiated condition and after the post-irradiation tempering. $R(Q)$ takes a nearly constant value of 2 approximately, which can be expected from Eq. (2) in the case of non-magnetic inhomogeneities imbedded in a fully magnetised martensitic matrix. Such inhomogeneities are tentatively identified as helium bubbles or, more likely, microvoids given the very low helium concentration expected under these irradiation conditions in this steel [12]; this interpretation, although consistent with what is known on the microstructural irradiation behaviour of such steels at such dose levels, should be experimentally confirmed by more detailed TEM analyses.

The growth of these inhomogeneities following post-irradiation treatment is shown also by a preliminary analysis of the size distributions of irradiated samples. Fig. 4 shows a comparison of the volume distributions corresponding to the SANS cross-sections of Fig. 3(a): the volume fraction of defects as small as 10 Å is almost one order of magnitude larger in the as-irradiated sample, while

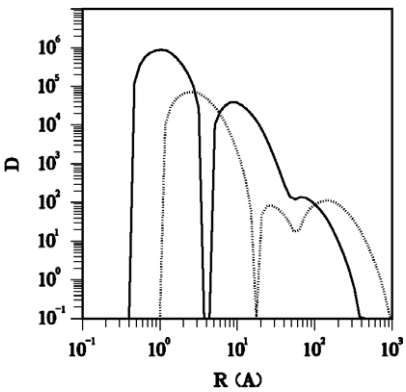

Fig. 4. Volume distribution functions $D(R)$ (in arbitrary units) vs. defect radius R (nm) for Optifer irradiated with 2.4 dpa at 250 °C (continuous line) and irradiated with 2.4 dpa at 250 °C then tempered 2 h at 770 °C (dotted line); the experimental error bands of such distributions, not reported in the picture, are 20% approximately.

defects one order of magnitude larger grow during post-irradiation tempering.

5. Conclusions

In the reduced activation Optifer steel neutron irradiation at 250 °C to a dose level of 0.8 dpa produces no detectable SANS effect; a subsequent tempering at 770 °C produces only a slight increase in the SANS cross-section, indicating an extremely low volume fraction of non-magnetic defects. After irradiation with 2.4 dpa a high density of small inhomogeneities is detected; a subsequent tempering at 770 °C appears to promote the growth of such defects to sizes one order of magnitude larger. Since these results refer to the difference in the SANS cross-sections of the irradiated and the reference samples, the observed SANS effect should not be attributed to defects arising from the thermal treatment but to the actual microstructural radiation damage; the SANS effect shown in Fig. 3 is therefore tentatively attributed to the growth of microvoids, although this interpretation has to be checked experimentally by other techniques.

References

[1] A. Hishinuma, A. Kohyama, R.L. Klueh, D.S. Gelles, W. Dietz, K. Ehrlich, J. Nucl. Mater. 258–263 (1998) 193.
[2] B.v.d. Schaaf, D.S. Gelles, S. Jitsukawa, A. Kimura, A. Möslang, G.R. Odette, J. Nucl. Mater. 283–287 (2000) 52.
[3] S. Jitsuawa, A. Kimura, A. Kohyama, R.L. Klueh, A.A. Tavassoli, B. van de Schaaf, G.R. Odette, J.W. Rensman, M. Victoria, C. Petersen, J. Nucl. Mater. 329–333 (2004) 39.
[4] L.A. Little, D.A. Stow, Met. Sci. 14 (1980) 14.
[5] E.A. Little, J. Nucl. Mater. 206 (1993) 324.
[6] R. Coppola, C. Dewhurst, R. Lindau, R.P. May, A. Möslang, M. Valli, Physica B 345 (2004) 225.
[7] R. Coppola, R. Lindau, M. Magnani, R.P. May, A. Möslang, J.W. Rensman, B. van der Schaaf, M. Valli, Fus. Eng. Des. 75–78 (2005) 985.
[8] R. Coppola, R. Lindau, M. Magnani, R.P. May, A. Möslang, M. Valli, Physica B 385–386 (2006) 647.
[9] R. Coppola, R. Lindau, M. Magnani, R.P. May, A. Möslang, M. Valli, Progress in Condensed Matter Physics, Nova Science Publisher Inc., in press.
[10] K. Ehrlich, S. Kelzenberg, H.D. Röhrig, L. Schäfer, M. Schirra, J. Nucl. Mater. 212–2005 (1994) 678.
[11] E. Materna-Morris, M. Rieth, K. Ehrlich, in: M.L. Hamilton et al. (Eds.), Proceedings of the 19 International Symposium in Effects of Radiation on Materials ASTM STP 1366, 1999, p. 597.
[12] M. Schirra, A. Falkenstein, S. Heger, J. Lapena, Creep and creep rupture properties of reduced activation martensitic OPTIFER alloys, Scientific Report FZKA-6464 (July 2001).
[13] G. Kostorz, in: W. Cahn, P. Haasen (Eds.), Neutron and X-ray Scattering Ch. 12 in Physical Metallurgy, 4th ed., 1996, p. 1115.
[14] M.T. Hutchings, C.G. Windsor, in: K. Sköld, D.L. Price (Eds.), Neutron Scattering, Methods of Experimental Physics, vol. 23-c, Academic Press, 1987, p. 405.
[15] R. Ghosh., S.U.Egelhaaf, A.R. Rennie (2006) ILL report ILL06GH05T.
[16] M. Magnani, P. Puliti, M. Stefanon, Nucl. Instrum. and Meth. A 271 (1988) 611.
[17] R. Coppola, R. Kampmann, M. Magnani, P. Staron, Acta Mater. 46 (1998) 5447.